NEUROSCIENCE

Neural network involving medial orbitofrontal cortex and dorsal periaqueductal gray regulation in human alcohol abuse

Tianye Jia[1,2,3]*†, Chao Xie[1,2]*, Tobias Banaschewski[4], Gareth J. Barker[5], Arun L. W. Bokde[6], Christian Büchel[7], Erin Burke Quinlan[3], Sylvane Desrivières[3], Herta Flor[8,9], Antoine Grigis[10], Hugh Garavan[11], Penny Gowland[12], Andreas Heinz[13], Bernd Ittermann[14], Jean-Luc Martinot[15], Marie-Laure Paillère Martinot[15,16], Frauke Nees[4,8,17], Dimitri Papadopoulos Orfanos[10], Luise Poustka[18], Juliane H. Fröhner[19], Michael N. Smolka[19], Henrik Walter[13], Robert Whelan[20], Gunter Schumann[1,21,22,23], Trevor W. Robbins[1,24]†, Jianfeng Feng[1,2,25,26,27]†, IMAGEN Consortium‡

Prompted by recent evidence of neural circuitry in rodent models, functional magnetic resonance imaging and functional connectivity analyses were conducted for a large adolescent population at two ages, together with alcohol abuse measures, to characterize a neural network that may underlie the onset of alcoholism. A network centered on the medial orbitofrontal cortex (mOFC), as well as including the dorsal periaqueductal gray (dPAG), central nucleus of the amygdala, and nucleus accumbens, was identified, consistent with the rodent models, with evidence of both inhibitory and excitatory coregulation by the mOFC over the dPAG. Furthermore, significant relationships were detected between raised baseline excitatory coregulation in this network and impulsivity measures, supporting a role for negative urgency in alcohol dependence.

INTRODUCTION

Alcohol use disorder (AUD) is a highly prevalent mental disorder characterized by harmful alcohol use (alcohol abuse) and alcohol dependence, according to both *Diagnostic and Statistical Manual of Mental Disorders, 5th Edition* (*DSM5*) (*1*) and *International Classification of Diseases 11th Revision* (*ICD-11*) (*2*) criteria. Hazardous alcohol use, e.g., binge drinking behavior, has been proposed as a risk factor for future AUD diagnosis (*2*–*4*). Multiple neurobiological mechanisms have been proposed for AUD, with particular emphases on reward-related, limbic, and prefrontal cortical regions (*5*).

Recently, modern neurobiological techniques, including optogenetics, have been used in animal models to elucidate the neural circuitry underlying possible precursors of alcohol dependence. For example, compulsive drinking by mice of alcohol adulterated with bitter-tasting quinine was bidirectionally modulated by activity in a novel circuitry involving direct projections from the medial prefrontal cortex (mPFC) to the brainstem dorsal periaqueductal gray (dPAG) (*6*), a region regulating both passive "freezing" versus active escape behaviors depending on the strength of aversive signals (*7*–*10*). According to this model, compulsive drinking arises because of a reduction in the influence of the mPFC and consequent disinhibition of the response to aversive stimuli. By contrast, a second study in rats has implicated the central nucleus of the amygdala (CeA) (*11*). Specifically, rats with deficits in the expression of the γ-aminobutyric acid (GABA) transporter GAT-3 preferred alcohol over a sweet solution, and animals normally preferring the sweet solution switched their preference to alcohol following knockdown of GAT-3. Furthermore, selective reductions in GAT-3 expression

[1]Institute of Science and Technology for Brain-Inspired Intelligence, Fudan University, Shanghai, China. [2]Key Laboratory of Computational Neuroscience and Brain-Inspired Intelligence (Fudan University), Ministry of Education, Shanghai, China. [3]Centre for Population Neuroscience and Precision Medicine (PONS), Institute of Psychiatry, Psychology and Neuroscience, SGDP Centre, King's College London, London SE5 8AF, UK. [4]Department of Child and Adolescent Psychiatry and Psychotherapy, Central Institute of Mental Health, Medical Faculty Mannheim, Heidelberg University, Square J5, 68159 Mannheim, Germany. [5]Department of Neuroimaging, Institute of Psychiatry, Psychology and Neuroscience, King's College London, London, UK. [6]Discipline of Psychiatry, School of Medicine and Trinity College Institute of Neuroscience, Trinity College Dublin, Dublin, Ireland. [7]University Medical Centre Hamburg-Eppendorf, Martinistr. 52, Hamburg, Germany. [8]Institute of Cognitive and Clinical Neuroscience, Central Institute of Mental Health, Medical Faculty Mannheim, Heidelberg University, Square J5, Mannheim, Germany. [9]Department of Psychology, School of Social Sciences, University of Mannheim, 68131 Mannheim, Germany. [10]NeuroSpin, C.E.A., Université Paris-Saclay, F-91191 Gif-sur-Yvette, France. [11]Departments of Psychiatry and Psychology, University of Vermont, Burlington, VT 05405, USA. [12]Sir Peter Mansfield Imaging Centre School of Physics and Astronomy, University of Nottingham, University Park, Nottingham, UK. [13]Department of Psychiatry and Psychotherapy, Charité–Universitätsmedizin Berlin, corporate member of Freie Universität Berlin, Humboldt-Universität zu Berlin, and Berlin Institute of Health, Berlin, Germany. [14]Physikalisch-Technische Bundesanstalt (PTB), Braunschweig and Berlin, Germany. [15]Institut National de la Santé et de la Recherche Médicale, INSERM U A10 "Trajectoires développementales en psychiatrie," Université Paris-Saclay, Ecole Normale supérieure Paris-Saclay, CNRS, Centre Borelli, Gif-sur-Yvette, France. [16]AP-HP.Sorbonne Université, Department of Child and Adolescent Psychiatry, Pitié-Salpêtrière Hospital, Paris, France. [17]Institute of Medical Psychology and Medical Sociology, University Medical Center Schleswig-Holstein, Kiel University, Kiel, Germany. [18]Department of Child and Adolescent Psychiatry and Psychotherapy, University Medical Centre Göttingen, von-Siebold-Str. 5, 37075 Göttingen, Germany. [19]Department of Psychiatry and Neuroimaging Center, Technische Universität Dresden, Dresden, Germany. [20]School of Psychology and Global Brain Health Institute, Trinity College Dublin, Dublin, Ireland. [21]PONS-Research Group, Charité Mental Health, Department of Psychiatry and Psychotherapy, Campus Charité Mitte, Berlin, Germany. [22]Department of Sports and Health Sciences, University of Potsdam, Potsdam, Germany. [23]PONS Centre, Institute for Science and Technology of Brain-inspired Intelligence (ISTBI), Fudan University, Shanghai, China. [24]Department of Psychology and Behavioural and Clinical Neuroscience Institute, University of Cambridge, Cambridge, UK. [25]School of Mathematical Sciences and Centre for Computational Systems Biology, Fudan University, Shanghai, China. [26]Department of Computer Science, University of Warwick, Coventry, UK. [27]Fudan ISTBI—ZJNU Algorithm Centre for Brain-inspired Intelligence, Zhejiang Normal University, Jinhua, China.
*These authors contributed equally to this work.
†Corresponding author. Email: tianyejia@fudan.edu.cn (T.J.); twr2@cam.ac.uk (T.W.R.); jianfeng64@gmail.com (J.F.)
‡Membership of the IMAGEN Consortium appears in the Supplementary Materials.

in the CeA were also found in people dying with AUD (*12*), helping to validate the importance of this murine model.

The question arises, however, of how to integrate these findings in the two murine models to define the neural circuitry contributing to the induction of alcohol dependence. It is well established, for example, that the CeA has a strong functional influence on the dPAG via its anatomical projections to regulate conditioned freezing behavior (*13*). Moreover, both the mPFC and the CeA that project into basal ganglia circuitry are also implicated in reward-related behavior and addiction (*14*) and are functionally interconnected themselves (*14*). Such broad connectivity between mPFC/orbitofrontal cortex (OFC) and subcortical regions has been well established and shown to be highly conserved across rodents and primates, including humans (*15*, *16*).

To address this key question of translational relevance to human alcohol abuse, we analyzed circuitry associated with alcohol abuse in the IMAGEN large sample (n = 1890) of adolescents. Previous functional magnetic resonance imaging (fMRI) studies in alcohol use mainly focused on either resting-state functional connectivities (rsFCs) (*17*–*21*) or task-based activations (*22*, *23*). For example, higher rsFCs involving the OFC have been associated with increased (*17*) and decreased (*21*) alcohol use in adolescents, whereas task-based activations have been almost exclusively of the ventral striatum (*22*, *23*). Here, we investigated this circuitry using both task-based FC (tbFC) and rsFC with a unified scheme in a longitudinal study, at ages 14 and 19 (*24*). We report that this analysis shows that the medial OFC (mOFC) and CeA are both implicated in a network, including the dPAG and the nucleus accumbens (NAcc), a structure implicated in reward processing.

By also using questionnaire data on the use of alcohol and impulsive behavior in this large sample, we were further able to formulate a novel hypothesis suggesting how compulsive drinking may arise via activity in this neural network.

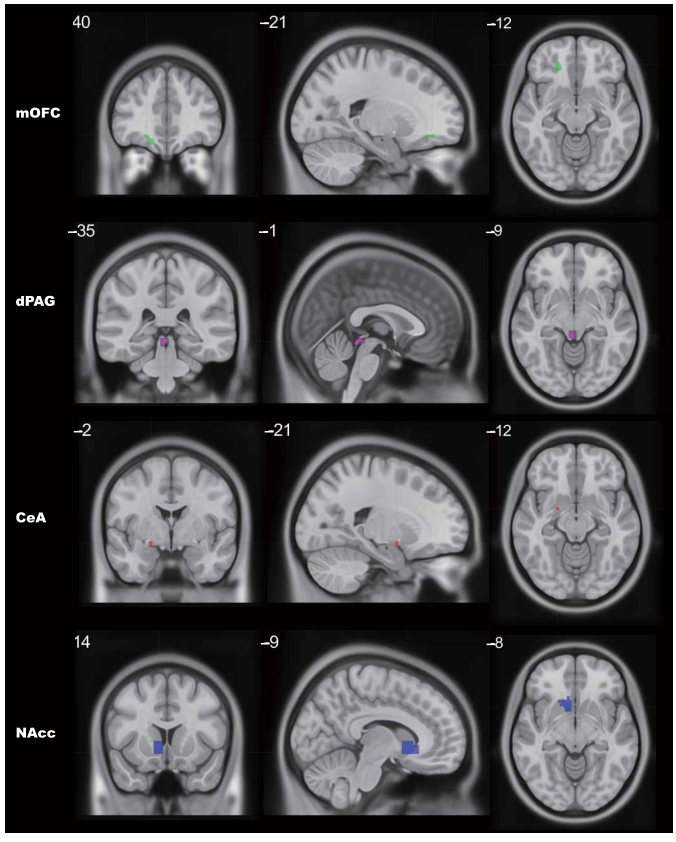

Fig. 1. Masks and MNI coordinates of mOFC, dPAG, CeA and NAcc. The masks of mOFC and dPAG were defined on the basis of the group-averaged activation (i.e., t statistics >5.0 during the feedback phase of contrast no-win versus large-win), while the templates for left NAcc and left CeA were derived from previous studies (*23*, *25*).

RESULTS

Task-based fMRI: Activations and FCs of reward and aversive signal processing networks during reward feedback

Nonreward (relative punishment) sensitivity of dPAG, mOFC, NAcc, and CeA during reward feedback

In a population of 1890 adolescent participants at age 14, we investigated the sensitivity to nonreward (i.e., relative punishment) by focusing on the "no-win versus large-win" (i.e., receiving an expected nonreward versus receiving an expected reward) contrast during the feedback phase of the monetary incentive delay (MID) task (fig. S1), and observed significant activations in the regions of interest (ROIs) normally implicated in processing reward-related signals, i.e., left mOFC (t = 8.7, Cohen's D = 0.20, and P < 0.001; Fig. 1) and left NAcc (t = 4.84, Cohen's D = 0.11, and P < 0.001; Fig. 1), and those specified for processing aversive signals (such as pain or fear), i.e., the dPAG (t = 5.2, Cohen's D = 0.12, and P < 0.001; Fig. 1) and the left CeA (t = 3.85, Cohen's D = 0.09, and P < 0.001; Fig. 1). Note that the ROIs for both dPAG and mOFC were defined on the basis of the group-averaged activations with nonreward sensitivity (i.e., the activation of no-win versus large-win) t statistics >5.0 during the feedback phase of the MID task. As only the left mOFC passed the significance threshold, the group-averaged templates for NAcc and CeA, derived from previous studies (*23*, *25*), also focused on the left hemisphere. Similar nonreward sensitivity was again observed for the same task in the same group of individuals at age 19 (n = 1242) for both dPAG (t = 3.5, Cohen's D = 0.10, and P < 0.001) and left mOFC (t = 7.3, Cohen's D = 0.21, and P < 0.001), but not for the left NAcc (t = 1.1, Cohen's D = 0.03, and P = 0.23) and left CeA (t = 0.1, Cohen's D = 0.00, and P = 0.91), which might suggest developmental changes in function for both NAcc and CeA during the reward feedback from ages 14 to 19.

Coregulation of activity within and between networks of reward and aversive signal processing

While all four ROIs were found to be activated during the contrast of no-win versus large-win at age 14 (n = 1852), we only observed significant positive tbFCs consistently across all experimental conditions within either the reward-signal processing network (i.e., between mOFC and NAcc: Cohen's D = 0.18, t = 7.89, and P < 0.001 at no-win; Cohen's D = 0.27, t = 11.56, and P < 0.001 at small-win; Cohen's D = 0.29, t = 12.40, and P < 0.001 at large-win; Fig. 2) or the aversive-signal processing network (i.e., between CeA and dPAG: Cohen's D = 0.07, t = 2.86, and P = 0.064 at no-win; Cohen's D = 0.09, t = 3.78, and P = 0.002 at small-win; Cohen's D = 0.11, t = 4.69, and P < 0.001 at large-win; Fig. 2). We also found significant negative tbFCs between these two networks (i.e., between mOFC and CeA: Cohen's D = −0.10, t = −4.52, and P < 0.001 at no-win; Cohen's D = −0.14, t = −5.94, and P < 0.001 at small-win; Cohen's D = −0.15, t = −6.29, and P < 0.001 at large-win; Fig. 2).

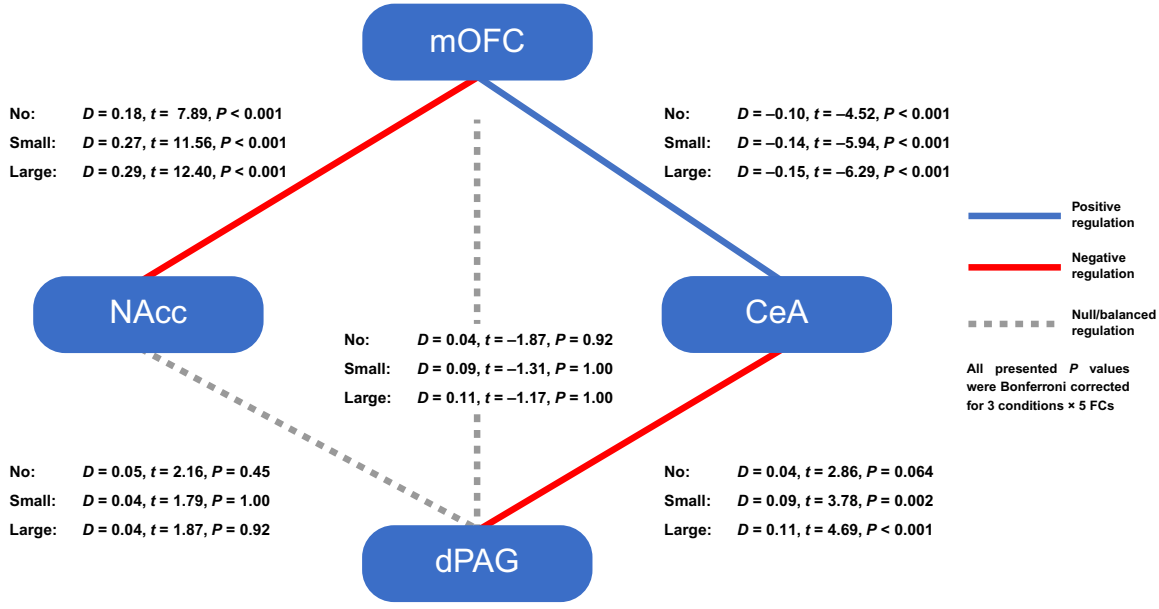

Fig. 2. FCs of reward/aversive signal processing networks at age 14.

These results, therefore, might suggest a generally inhibitory regulation between the reward and aversive signal processing networks (i.e., with negative tbFC), as well as an excitatory regulation within each network (i.e., with positive tbFC). The negative, although nonsignificant, tbFCs between mOFC and dPAG (Fig. 2) might represent relatively balanced excitatory and inhibitory regulation between mPFC and dPAG as observed in mice (*6*). At age 19, there were mostly nonsignificant tbFCs within and between these two networks, except for the mOFC-NAcc tbFC (fig. S2), which is likely due to a combined effect from both the reduced sample size (i.e., from 1852 to 1198) and the altered function of both NAcc and CeA during reward feedback, as shown above. All *P* values above were Bonferroni corrected for multiple comparisons (i.e., 3 conditions × 5 tbFCs).

Task-based fMRI: FC of reward and aversive signal processing networks during reward feedback and its association with alcohol abuse (a human validation of recent findings from animal models)

Strengthened mOFC-dPAG inhibition during reward feedback relates to higher alcohol abuse at both ages 14 and 19

Figure 3 shows that upon receiving nonreward, individuals with higher alcohol abuse scores [the Alcohol Use Disorders Identification Test (AUDIT)] showed strengthened negative mOFC-dPAG tbFC at age 14 ($r = -0.09$, $n = 1852$, $t = -4.07$, and $P < 0.001$), as well as at age 19 with an even stronger effect size ($r = -0.11$, $n = 1198$, $t = -3.93$, and $P < 0.001$), indicating a consistent underlying inhibitory regulation of mOFC over dPAG during no-reward feedback in the alcohol abusers, in contrast to the balanced regulation at the population level as shown above. Gender and research sites were included as control variables throughout the analysis unless otherwise specified. These findings are all highly consistent with those of Siciliano *et al.* (*6*), that suppressing mPFC signals to the PAG in mice produced compulsive alcohol drinking, and stronger inhibitory mPFC-PAG neuron response during early alcohol exposure is an early marker for later alcohol abuse. No significant association with alcohol abuse score was observed for mOFC-dPAG tbFC under both small-win and large-win conditions (table S1). All *P* values above were Bonferroni corrected for multiple comparisons (i.e., 3 conditions × 5 tbFCs × 2 time points). Despite similar associations between mOFC-dPAG tbFCs (upon receiving no-reward) and alcohol abuse scores being observed at both ages 14 and 19, as well as the small to medium correlation between alcohol abuse scores at both ages ($r = 0.23$, $n = 1398$, $t = 8.72$, and $P < 0.001$), no longitudinal correlation was observed between the mOFC-dPAG tbFCs measured at both ages ($r = -0.01$, $n = 1032$, $t = -0.27$, and $P = 0.789$; equivalence test for null effect: $P = 0.002$ for $r_L = -0.10$ and $P < 0.001$ for $r_U = 0.10$). It is notable that while lower mOFC-dPAG tbFC at age 14 did show a significant association with higher alcohol abuse scores at age 19 ($r = -0.052$, $n = 1198$, $t = -1.80$, and $P_{\text{one-tailed}} = 0.036$), this association was no longer significant when the alcohol abuse score at age 14 was controlled ($r = -0.031$, $n = 1198$, $t = -1.068$, and $P_{\text{one-tailed}} = 0.142$). These results may therefore indicate that the mOFC-dPAG tbFC only associates with current alcohol abuse status. In the gender-stratified analyses, the associations between higher alcohol abuse score and lower mOFC-dPAG tbFCs remained significant in both boys and girls separately at both age 14 ($r = -0.10$, $n = 914$, $t = -3.05$, and $P_{\text{uncorrected}} = 0.002$ in boys; $r = -0.09$, $n = 938$, $t = -2.71$, and $P_{\text{uncorrected}} = 0.007$ in girls) and 19 ($r = -0.13$, $n = 563$, $t = -3.01$, and $P_{\text{uncorrected}} = 0.003$ in boys; $r = -0.10$, $n = 635$, $t = -2.63$, and $P_{\text{uncorrected}} = 0.009$ in girls), without significant gender differences (test for difference between correlations: $z = 0.26$ and $P = 0.795$ at age 14, and $z = 0.50$ and $P = 0.617$ at age 19).

A further investigation into the subcategory of the alcohol abuse score from AUDIT showed that at both ages 14 ($n = 1852$) and 19 ($n = 1198$), the mOFC-dPAG tbFC during nonreward feedback associated with the indicative "hazardous alcohol use" (e.g., high frequency and quantity of alcohol use) (age 14: $r = -0.09$, $t = -3.67$, and $P_{\text{uncorrected}} < 0.001$, and age 19: $r = -0.12$, $t = -4.16$, and $P_{\text{uncorrected}} < 0.001$) and "harmful alcohol use" (e.g., alcohol blackout or injuries due to alcohol abuse) (age 14: $r = -0.08$, $t = -3.56$,

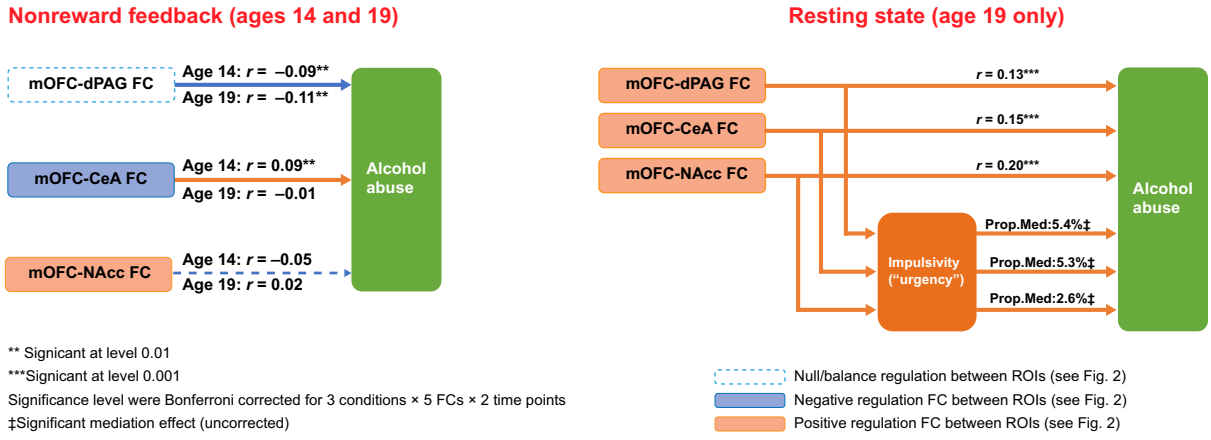

Fig. 3. The summary of the main findings.

$P_{uncorrected} < 0.001$, and age 19: $r = -0.09$, $t = -3.04$, and $P_{uncorrected} = 0.002$), whereas the association with severe alcoholic symptoms (i.e., "dependence symptoms") was only observed at age 19 ($r = -0.06$, $t = -2.03$, and $P_{uncorrected} = 0.043$) (table S2). See table S2 for the associations of mOFC-dPAG tbFC and each AUDIT subitem.

Weakened mOFC-CeA inhibition during reward feedback associated with greater alcohol abuse at age 14 but not 19

Upon receiving nonreward, individuals with higher alcohol abuse scores were found with weakened negative (i.e., a larger but still negative value) mOFC-CeA tbFC ($r = 0.09$, $t = 3.79$, and $P < 0.001$ Bonferroni corrected for 3 conditions × 5 FCs × 2 time points) at age 14 ($n = 1852$) (Fig. 3), suggesting that a reduced coregulation among mOFC and CeA upon receiving nonreward may contribute to alcohol abuse symptoms. This association was primarily observed in boys ($r = 0.12$, $n = 914$, $t = 3.78$, and $P_{uncorrected} < 0.001$) but not in girls ($r = 0.05$, $n = 938$, $t = 1.45$, and $P_{uncorrected} = 0.148$), although such a difference was not significant ($z = 1.67$ and $P = 0.095$). On the other hand, the same associations were practically null at age 19 ($P_{uncorrected} > 0.50$; equivalence test for null effect: $P < 0.001$ for both $r_L = -0.10$ and $r_U = 0.10$; Fig. 3), and we also failed to observe any association between the mOFC-CeA tbFC at age 14 and future alcohol abuse score at age 19 ($P_{uncorrected} > 0.80$; equivalence test for null effect: $P < 0.001$ for both $r_L = -0.10$ and $r_U = 0.10$). The diminished association with alcohol abuse at age 19 was in line with the reduced strength of the mOFC-CeA tbFC, as well as the inactivation for the corresponding CeA at age 19 as shown above. Further, we observed no significant associations between the mOFC-CeA tbFC with alcohol abuse at other experimental conditions, i.e., receiving a small or large reward, at both ages 14 and 19 (table S1).

A further investigation showed that, at age 14, the mOFC-CeA tbFC during nonreward feedback was associated with the indicative "hazardous use" ($r = 0.07$, $t = 3.08$, and $P_{uncorrected} = 0.002$), as well as with alcoholic "dependence symptoms" ($r = 0.05$, $t = 2.09$, and $P_{uncorrected} = 0.037$) and harmful alcohol use ($r = 0.09$, $t = 3.92$, and $P_{uncorrected} < 0.001$) (table S2). See table S2 for associations of mOFC-CeA tbFC with each AUDIT subitem at age 14.

It is notable that the tbFCs of mOFC-dPAG and mOFC-CeA during nonreward feedback at age 14 provide nonoverlapping significant contributions to the alcohol abuse score, i.e., remaining significant while mutually controlling each other in the same linear model ($r = -0.09$, $t = -3.94$, and $P < 0.001$ and $r = 0.08$, $t = 3.65$, and $P < 0.001$, respectively) (table S3). However, for CeA-dPAG, NAcc-dPAG, and mOFC-NAcc tbFCs, we observed no significant association with the alcohol abuse score across all reward conditions at both ages 14 and 19 (table S1).

Resting-state fMRI: FC of reward and aversive signal processing networks during resting-state and its association with alcohol abuse (an exploratory analysis outside the reward/punishment context)

Strengthened positive rsFCs among reward and aversive signal processing networks relate to greater alcohol abuse

At age 19, there was a strong positive rsFC between each pair of ROIs among both networks (minimum Cohen's $D > 0.5$, $P < 0.001$, and $n = 961$; see table S4) during resting-state fMRI. This contrasted with the situation during reward feedback where rsFCs among reward and aversive signal processing networks were largely nonsignificant, except for the mOFC-NAcc rsFC (fig. S2). In addition, higher alcohol abuse scores were found in significant association with increased strength of three out of five rsFCs ($n = 961$), i.e., the rsFCs linking mOFC with each of NAcc ($r = 0.20$, $t = 6.19$, and $P < 0.001$), CeA ($r = 0.15$, $t = 4.65$, and $P < 0.001$), and dPAG ($r = 0.13$, $t = 4.06$, and $P < 0.001$) (Fig. 3). These P values were corrected for the number of tested FCs. In the gender-stratified analyses, all three rsFCs remained significant when tested for associations with alcohol abuse scores in boys ($n = 447$; mOFC-NAcc: $r = 0.17$, $t = 3.53$, and $P_{uncorrected} < 0.001$; mOFC-CeA: $r = 0.18$, $t = 3.95$, and $P_{uncorrected} < 0.001$; mOFC-dPAG: $r = 0.11$, $t = 2.43$, and $P_{uncorrected} = 0.016$) and girls ($n = 514$; mOFC-NAcc: $r = 0.18$, $t = 4.09$, and $P_{uncorrected} < 0.001$; mOFC-CeA: $r = 0.11$, $t = 2.47$, and $P_{uncorrected} = 0.014$; mOFC-dPAG: $r = 0.13$, $t = 2.91$, and $P_{uncorrected} = 0.004$) separately, and there are no significant gender differences for these associations (mOFC-NAcc: $z = -0.19$ and $P = 0.85$; mOFC-CeA: $z = 0.13$ and $P = 0.21$; mOFC-dPAG: $z = -0.2$ and $P = 0.84$).

Further investigation showed that at age 19, the mOFC-related rsFCs were all associated with the indicative hazardous use ($n = 961$) (CeA: $r = 0.16$, $t = 4.95$, and $P_{uncorrected} < 0.001$; NAcc: $r = 0.20$, $t = 6.29$, and $P_{uncorrected} < 0.001$; and dPAG: $r = 0.12$, $t = 3.72$, and $P_{uncorrected} < 0.001$) and harmful alcohol use (CeA: $r = 0.09$, $t = 2.84$, and $P_{uncorrected} < 0.001$; NAcc: $r = 0.14$, $t = 4.23$, and $P_{uncorrected} < 0.001$; and dPAG: $r = 0.11$, $t = 3.40$, and $P_{uncorrected} < 0.001$), but not with

dependence symptoms (table S5). See table S5 for associations of mOFC-CeA, mOFC-NAcc, and mOFC-dPAG rsFCs with each AUDIT subitem at age 19.

rsFCs show overlapping contributions to alcohol abuse independent of the contribution from tbFC

A further multiple linear model integrating all these rsFCs could explain 3.2% variance of alcohol abuse scores at age 19 [adj-R^2 = 0.032, $F_{(5,955)}$ = 7.35, and P < 0.001], where only the mOFC-NAcc FC remained significant after controlling for the other rsFCs (r = 0.17, t = 3.16, and P = 0.002; table S6A), suggesting a commonly shared variance of alcohol abuse scores among all rsFCs, although dominated by the mOFC-NAcc rsFC.

In addition, the tbFC of mOFC-dPAG at age 19, as identified above, could explain an additional 1% variance above the rsFCs (t = −3.27 and P = 0.001), increasing the total explained variance to 4.4% [adj-R^2 = 0.044, $F_{(6,906)}$ = 7.97, and P < 0.001; table S6B]. Therefore, tbFC and rsFC from the reward and aversive signal processing networks may contribute independently to alcohol abuse, thus representing different underlying neural mechanisms.

Impulsivity partially mediates the associations between rsFCs and alcohol abuse

Impulsivity, especially "urgency," has been consistently proposed as a major risk factor for alcohol abuse (*26*, *27*). Collectively, rsFCs from mOFC (i.e., mOFC-dPAG, mOFC-NAcc, and mOFC-CeA) were found to be in significant associations with the impulsivity total score [measured by the temperament and character inventory (TCI)] [adj-R^2 = 0.009, $F_{(3,947)}$ = 2.65, and P = 0.047], particularly the subitem representing urgency: "I like to make quick decisions so I can get on with what has to be done" [adj-R^2 = 0.009, $F_{(3,947)}$ = 3.89, and $P_{\text{uncorrected}}$ = 0.009]. All three mOFC-related rsFCs also showed significant associations with this item in the corresponding univariate analyses (n = 951) (CeA: r = 0.10, t = 2.96, and $P_{\text{uncorrected}}$ = 0.003; NAcc: r = 0.07, t = 2.10, and $P_{\text{uncorrected}}$ = 0.040; dPAG: r = 0.08, t = 2.58, and $P_{\text{uncorrected}}$ = 0.009). Mediation analyses further suggested that the urgency subitem may act as an intermediary variable in the link between the mOFC-related rsFCs and the alcohol abuse: mOFC-related FCs→impulsivity→AUDIT total score [CeA: proportion mediated (Prop.Med.) = 5.3%; 95% confidence interval (CI), 0.01 to 0.13; and P= 0.014; NAcc: Prop.Med. = 2.6%; 95% CI, 0.001 to 0.07; and P = 0.034; dPAG: Prop.Med. = 5.4%; 95% CI, 0.007 to 0.15; and P = 0.014; Fig. 3). In contrast, this urgency subitem showed no association with the mOFC-PAG tbFC (nonreward feedback) (r = −0.01, n = 1164, t = −0.48, and P = 0.646; equivalence test for null effect: P = 0.002 for r_L = −0.10 and P < 0.001 for r_U = 0.10) at age 19, and so did the impulsivity total score (r = 0.02, n = 1164, t = 0.63, and P = 0.523; equivalence test for null effect: P < 0.001 for r_L = −0.10 and P = 0.003 for r_U = 0.10), suggesting that the mediating role of impulsivity was specific to rsFCs.

Impacts of other substance use and psychiatric symptoms on relationships of both tbFC and rsFC with alcohol abuse

As alcohol abuse is commonly comorbid with other substance abuse and psychiatric disorders, we further investigated whether these factors could confound our findings. In the present sample, we first confirmed that alcohol abuse scores were highly correlated with other substance use (i.e., yearly cannabis use and monthly smoking) and common psychiatric symptoms [i.e., depression, anxiety, attention deficit hyperactivity disorder (ADHD) symptoms, and conduct problems] (table S7A).

We then checked for possible associations between the identified tbFC and rsFC and the other substance use/psychiatric symptoms, and we found the following results: at age 14, neither task-based mOFC-CeA FC nor task-based mOFC-dPAG FC was found to be strongly associated with other substance use and psychiatric symptoms (i.e., all $P_{\text{uncorrected}}$ > 0.05; equivalence tests for null effects: P_{max} = 0.005 for r_L = −0.10 and P_{max} = 0.003 for r_U = 0.10; table S7, B and C); at age 19, the tbFC of mOFC-dPAG showed nominally significant association with cannabis use (r = −0.06, n = 1193, t = −2.04, and $P_{\text{uncorrected}}$ = 0.042) and smoking (r = −0.07, n = 1193, t = −2.28, and $P_{\text{uncorrected}}$ = 0.023) (table S7D). However, neither association was significant when controlling for alcohol abuse scores (for cannabis use: r = −0.02, t = −0.82, and $P_{\text{uncorrected}}$ = 0.418; for smoking: r = −0.04, t = −1.28, and $P_{\text{uncorrected}}$ = 0.204), suggesting both cannabis use and smoking were secondary to alcohol abuse in terms of their associations with the tbFC of mOFC-dPAG. Also, at age 19, we found the rsFC of mOFC-NAcc in a nominally significant association with cannabis use (r = 0.08, n = 956, t = 2.37, and $P_{\text{uncorrected}}$ = 0.018), ADHD symptoms (r = 0.09, n = 951, t = 2.69, and $P_{\text{uncorrected}}$ = 0.007), and conduct problems (r = 0.09, n = 951, t = 2.63, and $P_{\text{uncorrected}}$ = 0.009) (table S7F). Again, these associations disappeared when controlling for alcohol abuse (for cannabis use: r = −0.01, n = 956, t = −0.23, and $P_{\text{uncorrected}}$ = 0.819; for ADHD symptoms: r = 0.05, n = 951, t = 1.59, and $P_{\text{uncorrected}}$ = 0.112; for conduct problems: r = 0.05, n = 951, t = 1.67, and $P_{\text{uncorrected}}$ = 0.097). The other two rsFCs had no significant association with the other substance use or psychiatric symptoms (table S7, E and G).

Last, after controlling for all of the other substance use and psychiatric symptoms, the significant associations of alcohol abuse score with both tbFC and rsFCs remained significant (tbFC mOFC-dPAG: r = −0.08, n = 1845, t = −3.37, and $P_{\text{uncorrected}}$ < 0.001 at age 14, and r = −0.08, n = 1051, t = −2.53, and $P_{\text{uncorrected}}$ = 0.012 at age 19; tbFC mOFC-CeA at age 14: r = 0.08, n = 1845, t = 3.61, and $P_{\text{uncorrected}}$ < 0.001; rsFC mOFC-dPAG at age 19: r = 0.13, n = 856, t = 3.96, and $P_{\text{uncorrected}}$ < 0.001; rsFC mOFC-CeA at age 19: r = 0.14, n = 856, t = 4.09, and $P_{\text{uncorrected}}$ < 0.001; rsFC mOFC-NAcc at age 19: r = 0.16, n = 856, t = 4.63, and $P_{\text{uncorrected}}$ < 0.001; also, see table S8 for more detailed results with AUDIT subcategories and items). Therefore, the above results indicate not only that the observed associations between tbFC and rsFC and alcohol abuse score were unlikely due to other confounding factors, such as substance abuse and psychiatric disorders, but also that these FCs were highly specific for alcohol abuse rather than abuse of other substances.

DISCUSSION

Analysis of FC in two neuroimaging modalities, task-based fMRI using the monetary delayed incentive task and resting-state fMRI, in a large population of human adolescents, was used successfully to support the neural validity of two distinct rodent models of AUD. In addition, further analysis revealed a possible role for impulsivity in causal mediation of the link with self-reported measures of alcohol abuse.

At age 14, we identified that mOFC upon receiving nonreward (relative punishment) regulates adolescent alcohol abuse via two distinct pathways: (i) an mOFC-dPAG tbFC inhibitory pathway involved in regulating the transmission of punishment signals, the inhibition of which was proposed to facilitate compulsive drinking behavior (*6*); (ii) an mOFC-CeA tbFC pathway involved in processing

negative emotion (*11*), in which greater negative emotion perception during no-reward feedback is linked to higher alcohol consumption.

At age 19, however, only the mOFC-dPAG tbFC inhibitory pathway remained significant, and the mOFC-CeA tbFC pathway was muted, potentially due to the significantly reduced tbFC strength at age 19 ($t = -2.11$, $n = 1032$, and $P = 0.035$). In addition, the same mOFC-dPAG FC during resting state was also identified to be in significant association with alcohol abuse, although in the opposite direction. These results, therefore, might suggest two independent regulatory pathways between mOFC and dPAG contributing to alcohol abuse, excitatory regulation during resting state, and inhibitory regulation upon receiving nonreward (relative punishment), given the observation that both excitatory and inhibitory neurons project from mPFC/mOFC to dPAG (*6*, *10*). While inhibiting transmission of punishment information to dPAG (i.e., aborting bottom-up regulation) plays a central role in the reduced sensitivity to the punishment that further leads to compulsive alcohol use, as suggested by Siciliano *et al.* (*6*), dPAG has also been found to have a top-down regulatory role in thresholding and initiating "escape" behavior by regulating its vigor and reaction time (*7*–*9*). Therefore, the excitatory regulation of mOFC over dPAG during resting state, which is not subject to a specific stimulus, may serve as an example of top-down regulation. Stronger coregulation between mOFC and dPAG during the resting state may indicate an elevated baseline excitation of dPAG neurons, which could not only produce persistent aversive signals but also lower the threshold of external stimuli to initiate escape behavior. The combination of both may cause impulsive responses known as "negative urgency," a consistently identified major risk factor for alcohol abuse (*26*, *27*). This hypothesis was supported by the significant mediation effect of the "urgency" item over the association between mOFC-dPAG rsFC and alcohol abuse (see Fig. 4 as a summary of both pathways). Also, both mOFC-NAcc and mOFC-CeA rsFCs may additionally affect alcohol abuse through (partly) regulating impulsive behaviors, which largely resemble the findings of mOFC-dPAG rsFC, hence suggesting a regulatory network of dPAG with a central focus at mOFC, and input from the amygdala and ventral striatum (*10*). The above findings might echo a previous case-control study of alcohol dependence (*28*) with a relatively small sample size (25 cases and 26 controls), where higher rsFCs were observed in the alcohol dependence group. However, these authors also found OFC-related rsFCs in negative correlations with negative urgency in the alcohol dependence group, in contrast to our finding that stronger OFC-related rsFCs were related to higher urgency, which is more consistent with the positive behavioral correlation between negative urgency and alcohol dependence (*26*, *27*).

To demonstrate these results, it has been necessary to analyze data from a large cohort of human adolescents, some of whom are at the onset of alcohol abuse, studied longitudinally. While many of the findings are highly significant, the amount of variance accounted for is inevitably small, indicating that many other factors, other than, for example, impulsivity and reductions in regulatory control over aversive processing, likely contribute to drinking in this population (*29*). The interpretation of the contrasting findings for the task-based and resting-state mOFC-dPAG FCs in relation to self-reported alcohol abuse in terms of an altered excitatory-inhibitory balance of mOFC outflow to the dPAG is hypothetical and requires further confirmation, but is consistent with our functional interpretation.

We further showed that common confounding factors, such as gender, other substance use, and psychiatric problems, have negligible impacts on the associations of both tbFC and rsFC with alcohol abuse. Also, while some FCs did show weak associations with other substance use or psychiatric problems, these associations did not survive after controlling for alcohol abuse. Together, these results suggested both tbFC and rsFC connecting mOFC to subcortical regions, i.e., NAcc, CeA, and dPAG, were highly specific for alcohol abuse rather than abuse of other substances. In line with this, while previous studies have shown that brain-wide increased rsFCs were correlated with higher alcohol use but lower smoking (*17*), such a phenomenon was not observed in either rsFC or tbFCs among our targeted ROIs. However, we also noted that other substance use, notably of tobacco and cannabis, was only moderate in the present cohort (Table 1), and hence, our findings might not be directly translated to cohorts with more severe other substance use. Nonetheless, our findings therefore probably relate more specifically to alcohol abuse. In addition, while the previous literature has found anticorrelations between the rsFC of mOFC-CeA and both the current and future alcohol use in adolescents (*21*, *30*), our findings instead indicate a positive correlation. Last, we concede that our findings were unable to predict future alcohol abuse, even though the same tbFC of mOFC-dPAG was found in association with alcohol abuse at both ages 14 and 19.

In summary, we report evidence that mOFC-dPAG activity is linked to alcohol abuse in humans, in line with the observation in mice, indicating that the findings in a mouse calcium imaging and optogenetic study of adulterated alcohol drinking (*6*) have relevance for human alcohol abuse. The current study highlighted the mOFC in humans rather than the agranular mPFC in mice, which is a possible limitation in any homologous comparison; however, both primate regions are intimately implicated in the medial visceromotor network (*31*). Moreover, we found that the CeA, which is also implicated in both rodent and human alcohol dependence (*11*), as well

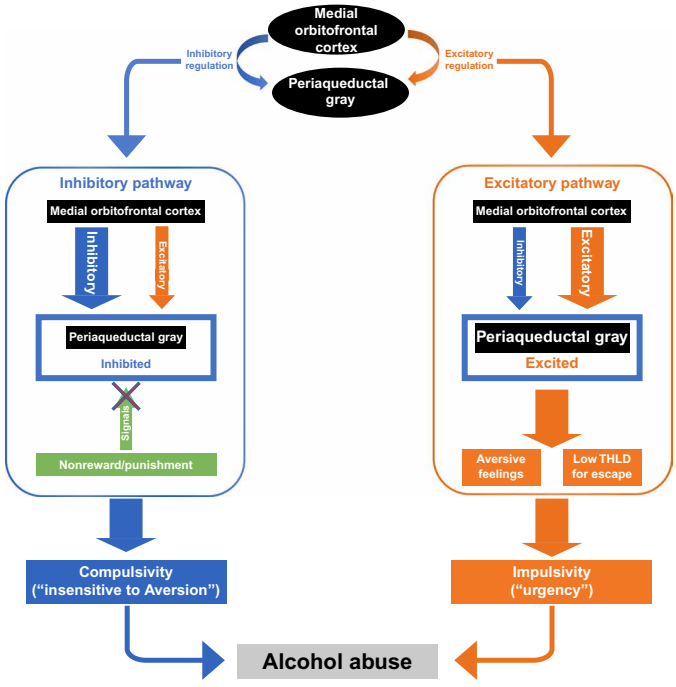

Fig. 4. Dual pathways of mOFC-PAG regulation that leads to alcohol abuse.

Table 1. Characteristics of the study population from the IMAGEN cohort. Individuals were flagged with "alcohol abuse" if they scored more than 7 on the total score of AUDIT (Alcohol Use Disorders Identification Test); individuals were flagged with "tobacco user" if they self-reported as smoking on a daily basis and "cannabis user" if they had at least one of either marijuana or hashish in the last year from the ESPAD (European School Survey Project on Alcohol and Other Drugs); individuals were flagged as "anxiety" or "depression" if they scored more than 4 (i.e., very likely) in the corresponding disorder bands (compatible with *ICD-10* or *DSM4*) on the basis of DAWBA (Development and Well-Being Assessment); individuals were flagged with high risk for "ADHD" (attention deficit hyperactivity disorder) or "conduct disorder" if they scored 7 and more for the hyperactivity score or scored 4 and more for the conduct problems score in self-reported SDQ (Strengths and Difficulties Questionnaire), respectively; smoking behavior was measured as the frequency (i.e., cigarettes per day) of smoking during the last 30 days, and cannabis use was measured as the number of times using either marijuana or hashish in the last year from the ESPAD. The mean values of quantitative measurements were calculated on the basis of the full sample.

Characteristic measurement	Baseline, age 14 ($N = 1890$)		Two-year follow-up, age 19 ($N = 1198$)	
Dichotomized measurements	***n***	**%**	***n***	**%**
Male	931	49.3	590	47.5
Alcohol abuse (AUDIT)	50	2.7	292	26.1
Tobacco user (ESPAD)	141	7.5	324	27.0
Cannabis user (ESPAD)	110	5.8	469	39.2
Depression (DAWBA)	22	1.1	42	3.9
Anxiety (DAWBA)	16	0.8	17	1.6
ADHD (SDQ)	240	12.8	97	8.1
Conduct disorder (SDQ)	146	7.8	39	3.2
Quantitative measurements	**Mean**	**SD**	**Mean**	**SD**
AUDIT total score	1.34	2.13	5.55	3.37
Hazardous use	1.08	1.53	4.54	2.33
Dependence symptoms	0.11	0.58	0.43	0.92
Harmful alcohol use	0.26	0.85	1.01	1.50
Impulsivity total score (TCI)	27.03	3.94	24.62	5.42
Smoking per day (ESPAD)	0.29	1.48	1.85	3.95
Cannabis use yearly (ESPAD)	0.59	3.88	6.72	12.74

as in control over escape behavior mediated by the dPAG (*13*), is also associated with the mOFC network. Hence, a major outcome of this study has been to translationally validate the two recent prominent murine studies of compulsive alcohol drinking. A second outcome has been to identify how different modes of interaction of the mOFC with the dPAG may modulate alcohol drinking via effects on impulsivity.

MATERIALS AND METHODS

Participants

Two thousand Caucasian adolescents from the IMAGEN project were included in the present study, with data collected from eight sites across Europe (i.e., France, United Kingdom, Ireland, and Germany). The project was approved by all local ethics research committees, and informed consent was obtained from participants and their parents/guardians. A detailed description of the study protocol and data acquisition has been previously published (*24*). In this study, we investigated individuals with matched neuroimaging and behavior data at baseline (age 14, $n = 1890$) and the follow-up (age 19, $n = 1242$).

Measurement of alcohol abuse and impulsive behaviors

The alcohol abuse behavior of the IMAGEN participants was assessed using the screening questions from the AUDIT (*3*). The AUDIT was developed by the World Health Organization as a simple way to screen and identify people who are at risk of developing alcohol problems. The AUDIT test focuses on identifying the preliminary signs of hazardous drinking, mild dependence, and harmful alcohol use (table S2). It is used to detect alcohol problems experienced within the last year. Individuals were flagged with "alcohol abuse" if they scored more than 7 on the total score of AUDIT. It is one of the most accurate alcohol screening tests available (*32*). The measurement of impulsive behavior was conducted through the TCI (*33*), which provides a reliable and meaningful description of individual personality.

Measurement of other substance use and psychiatric symptoms

The measurements of substance use of the IMAGEN participants were based on the European School Survey Project on Alcohol and Other Drugs (ESPAD; http://espad.org/), one of the largest cross-national research projects on adolescent substance use in the world. In the present study, we focused on two substance use behaviors: smoking and cannabis use. Smoking behavior was measured as the frequency during the last 30 days (How frequently have you smoked cigarettes during the LAST 30 DAYS, cigarettes per day?), and cannabis use was measured as the quantity of marijuana or hashish in the last year [How many occasions OVER THE LAST 12 MONTHS have you used marijuana (grass and pot) or hashish (hash and hash oil)?].

The depression and anxiety symptoms of the IMAGEN participants were assessed with the Development and Well-Being Assessment (DAWBA) (*34*), which is a wide-ranging psychiatric screening questionnaire and has previously been used to define subthreshold clinical symptoms in neuroimaging studies of subclinical psychopathology (*35*). The participants were flagged as "anxiety" or "depression" if they scored more than 4 (i.e., very likely) in the corresponding disorder bands (compatible with *ICD-10* or *DSM4*) based on DAWBA. The symptoms of ADHD and conduct disorder were assessed with the self-reported hyperactivity score and conduct problems score, respectively, from the Strengths and Difficulties Questionnaire (SDQ) (*34*). The self-reported SDQ was used for both ADHD and conduct disorders because it is the only available questionnaire/assessment that could provide consistent investigations at both ages 14 and 19. The participants were labeled as high risk for ADHD or conduct disorder if they scored 7 and more for the hyperactivity score or 4 and more for conduct problems score.

MID task

Participants performed a modified version of the MID task to examine neural responses to reward anticipation and reward outcome (*36*). The task consisted of 66 10-s trials. In each trial, participants were presented with one of three cue shapes (cue, 250 ms), denoting whether a target (white square) would subsequently appear on the left or right side of the screen and whether 0, 2, or 10 points could be won in that trial. After a variable delay (4000 to 4500 ms) of fixation on a white crosshair, participants were instructed to respond with left/right button press as soon as the target appeared. Feedback on whether and how many points were won during the trial was presented for 1450 ms after the response. With a tracking algorithm, task difficulty (i.e., target duration varied between 100 and 300 ms) was individually adjusted, such that each participant successfully responded on ~66% of trials. Participants had first completed a practice session outside the scanner (~5 min), during which they were instructed that for every 5 points won, they would then receive one food snack in the form of small chocolate candies at age 14 or a small amount of cash at age 19. The current study focused on task conditions during the feedback phase and consisted of only hit trials where the participants successfully hit the target before it disappeared.

fMRI data acquisition and preprocessing

Image acquisition

Functional MRI data were acquired at eight IMAGEN assessment sites with 3-T MRI scanners of different manufacturers (Siemens, Philips, General Electric, Bruker). The scanning variables were specifically chosen to be compatible with all scanners. The same scanning protocol was used in all sites. In brief, high-resolution T1-weighted three-dimensional structural images were acquired for anatomical localization and coregistration with the functional time series. Blood oxygen level–dependent (BOLD) functional images were acquired with gradient-echo, echo-planar imaging (EPI) sequence. For any tasks, 300 volumes were acquired for each participant, and each volume consisted of 40 slices aligned to the anterior commission/posterior commission line (2.4-mm slice thickness and 1-mm gap). The echo time (TE) was optimized [TE = 30 ms, repetition time (TR) = 2200 ms] to provide reliable imaging of subcortical areas.

Task-based functional image preprocessing

Task-based functional MRI data were first analyzed with SPM12 (Statistical Parametric Mapping, http://fil.ion.ucl.ac.uk/spm). Spatial preprocessing included the following: slice time correction to adjust for time differences due to multislice imaging acquisition, realignment to the first volume in line, nonlinearly warping to the Montreal Neurological Institute (MNI) space [based on a custom EPI template ($53 \times 63 \times 46$ voxels) created out of an average of the mean images of 400 adolescents], resampling at a resolution of $3 \times 3 \times 3\text{mm}^3$, and smoothing with an isotropic Gaussian kernel of 5-mm full-width at half-maximum (FWHM).

Resting-state functional image preprocessing

The resting-state image was processed with suggested protocols from Functional Magnetic Resonance Imaging of the Brain (FMRIB's) Software Library (FSL v5.0.9) and Advanced Normalization Tools (ANTs v1.9.2): Motion correction was carried out by applying a rigid-body registration of each volume to the middle volume (FSL MCFLIRT); nonbrain tissue was removed (FSL BET); and spatial smoothing was applied using a 4-mm FWHM Gaussian kernel. Independent component analysis (FSL MELODIC) was run for each dataset. Artifact components were identified using an automatic classification algorithm and subsequently regressed out from the data (ICA-AROMA v0.3) (*37*). The hence cleaned data were then detrended, up to a third-degree polynomial, coregistered to a high-resolution T1 image [the Boundary-Based Registration (BBR) algorithm used by FSL FLIRT], and normalized to 2-mm isotropic MNI standard space (ANTs). At last, the preprocessed and normalized resting-state data were resliced to 3-mm isotropic voxels. With the preprocessed data, we calculated Pearson correlations between the extracted mean time courses of provided ROI masks, of which the Fisher *z*-transformation was applied to calculate the rsFCs.

Activation and FC of task-based fMRI

At the first-level analysis, the BOLD signal for each subject was assessed by a linear combination of 12 regressors for experimental conditions, i.e., 2 targets (hit and miss) × 2 phases (anticipation and feedback) × 3 reward magnitudes (no-win, small-win, and large-win), where the regressor modeling each of the experimental conditions was established by convolving the corresponding experimental condition with SPM's canonical hemodynamic response function. The final general linear model (GLM) contained 12 task-condition regressors and 21 covariate regressors consisting of 12 motion regressors (3 translations, 3 rotations, 3 translations shifted 1 TR before, and 3 translations shifted 1 TR later) and 9 additional columns corresponding to the long-term effects of the movement [3 nuisance variables for the white matter and 6 nuisance variables for ventricles, and commonly referred to as CompCor correction (*38*)]. These regressors were used with the SPM to estimate the condition-specific brain activation, i.e., the regression coefficient of the corresponding task-condition regressor in the GLM.

The CONN toolbox (*39*) (version 16.h) was used to estimate the condition-specific FC (i.e., no-win, small-win, and large-win) with the weighted GLM (wGLM) method. Twelve task-condition regressors and 21 covariate regressors derived above were first regressed out from the raw BOLD signal of each ROI, and the residual signals were further fed into wGLMs to investigate conditional time series correlations (i.e., the conditional FC) between any pairs of ROIs, where the temporal weight function for each condition was calculated as the corresponding but now rectified task-condition regressor (i.e., only time points expected with positive BOLD signals count). This approach amplifies the expected hemodynamic delay to each task condition and deweights the initial and final scans when

estimating functional correlation measures to avoid spurious jumps in BOLD signals, as well as reducing the potential cross-talk between adjacent task conditions (*39*). Following the above procedure, ROI-to-ROI conditional FCs were established, where the group-averaged mask templates of ROIs were obtained either from the above activation analyses (i.e., dPAG and mOFC) or based on previous studies (i.e., CeA and NAcc) (*23*, *25*).

SUPPLEMENTARY MATERIALS

Supplementary material for this article is available at http://advances.sciencemag.org/cgi/content/full/7/6/eabd4074/DC1

REFERENCES AND NOTES

1. B. F. Grant, R. B. Goldstein, T. D. Saha, S. P. Chou, J. Jung, H. Zhang, R. P. Pickering, W. J. Ruan, S. M. Smith, B. Huang, D. S. Hasin, Epidemiology of DSM-5 alcohol use disorder. *JAMA Psychiat.* **72**, 757–766 (2015).
2. J. B. Saunders, L. Degenhardt, G. M. Reed, V. Poznyak, Alcohol use disorders in ICD-11: Past, present, and future. *Alcohol. Clin. Exp. Res.* **43**, 1617–1631 (2019).
3. J. P. Allen, R. Z. Litten, J. B. Fertig, T. Babor, A review of research on the Alcohol Use Disorders Identification Test (AUDIT). *Alcohol. Clin. Exp. Res.* **21**, 613–619 (1997).
4. G. Addolorato, G. A. Vassallo, G. Antonelli, M. Antonelli, C. Tarli, A. Mirijello, A. Agyei-Nkansah, M. C. Mentella, D. Ferrarese, V. Mora, M. Barbàra, M. Maida, C. Cammà, A. Gasbarrini; Alcohol Related Disease Consortium, Binge drinking among adolescents is related to the development of alcohol use disorders: Results from a cross-sectional study. *Sci. Rep. Uk* **8**, 12624 (2018).
5. C. Cui, A. Noronha, H. Morikawa, V. A. Alvarez, G. D. Stuber, K. K. Szumlinski, T. L. Kash, M. Roberto, M. V. Wilcox, New insights on neurobiological mechanisms underlying alcohol addiction. *Neuropharmacology* **67**, 223–232 (2013).
6. C. A. Siciliano, H. Noamany, C. J. Chang, A. R. Brown, X. Chen, D. Leible, J. J. Lee, J. Wang, A. N. Vernon, C. M. Vander Weele, E. Y. Kimchi, M. Heiman, K. M. Tye, A cortical-brainstem circuit predicts and governs compulsive alcohol drinking. *Science* **366**, 1008–1012 (2019).
7. D. A. Evans, A. V. Stempel, R. Vale, S. Ruehle, Y. Lefler, T. Branco, A synaptic threshold mechanism for computing escape decisions. *Nature* **558**, 590–594 (2018).
8. P. Tovote, M. S. Esposito, P. Botta, F. Chaudun, J. P. Fadok, M. Markovic, S. B. Wolff, C. Ramakrishnan, L. Fenno, K. Deisseroth, C. Herry, S. Arber, A. Luthi, Midbrain circuits for defensive behaviour. *Nature* **534**, 206–212 (2016).
9. Y. Lefler, D. Campagner, T. Branco, The role of the periaqueductal gray in escape behavior. *Curr. Opin. Neurobiol.* **60**, 115–121 (2019).
10. J. L. Price, Free will versus survival: Brain systems that underlie intrinsic constraints on behavior. *J. Comp. Neurol.* **493**, 132–139 (2005).
11. E. Augier, E. Barbier, R. S. Dulman, V. Licheri, G. Augier, E. Domi, R. Barchiesi, S. Farris, D. Natt, R. D. Mayfield, L. Adermark, M. Heilig, A molecular mechanism for choosing alcohol over an alternative reward. *Science* **360**, 1321–1326 (2018).
12. M. Heilig, E. Augier, S. Pfarr, W. H. Sommer, Developing neuroscience-based treatments for alcohol addiction: A matter of choice? *Transl. Psychiatry* **9**, 255 (2019).
13. M. L. Brandão, T. A. Lovick, Role of the dorsal periaqueductal gray in posttraumatic stress disorder: Mediation by dopamine and neurokinin. *Transl. Psychiatry* **9**, 232 (2019).
14. D.-O. Seo, S. C. Funderburk, D. L. Bhatti, L. E. Motard, D. Newbold, K. S. Girven, J. G. McCall, M. Krashes, D. R. Sparta, M. R. Bruchas, A GABAergic projection from the centromedial nuclei of the amygdala to ventromedial prefrontal cortex modulates reward behavior. *J. Neurosci.* **36**, 10831–10842 (2016).
15. D. E. Moorman, The role of the orbitofrontal cortex in alcohol use, abuse, and dependence. *Prog. Neuro-Psychopharmacol. Biol. Psychiatry* **87**, 85–107 (2018).
16. S. R. Heilbronner, J. Rodriguez-Romaguera, G. J. Quirk, H. J. Groenewegen, S. N. Haber, Circuit-based corticostriatal homologies between rat and primate. *Biol. Psychiatry* **80**, 509–521 (2016).
17. W. Cheng, E. T. Rolls, T. W. Robbins, W. Gong, Z. Liu, W. Lv, J. Du, H. Wen, L. Ma, E. B. Quinlan, H. Garavan, E. Artiges, D. Papadopoulos Orfanos, M. N. Smolka, G. Schumann, K. Kendrick, J. Feng, Decreased brain connectivity in smoking contrasts with increased connectivity in drinking. *eLife* **8**, (2019).
18. V. M. Vergara, J. Liu, E. D. Claus, K. Hutchison, V. Calhoun, Alterations of resting state functional network connectivity in the brain of nicotine and alcohol users. *NeuroImage* **151**, 45–54 (2017).
19. S. J. Fede, E. N. Grodin, S. F. Dean, N. Diazgranados, R. Momenan, Resting state connectivity best predicts alcohol use severity in moderate to heavy alcohol users. *NeuroImage* **22**, 101782 (2019).
20. A. Cservenka, K. Casimo, D. A. Fair, B. J. Nagel, Resting state functional connectivity of the nucleus accumbens in youth with a family history of alcoholism. *Psychiatry Res.* **221**, 210–219 (2014).
21. S. Peters, D. J. Jolles, A. C. Van Duijvenvoorde, E. A. Crone, J. S. Peper, The link between testosterone and amygdala-orbitofrontal cortex connectivity in adolescent alcohol use. *Psychoneuroendocrinology* **53**, 117–126 (2015).
22. I. M. Balodis, M. N. Potenza, Anticipatory reward processing in addicted populations: A focus on the monetary incentive delay task. *Biol. Psychiatry* **77**, 434–444 (2015).
23. T. Jia, C. Macare, S. Desrivieres, D. A. Gonzalez, C. Tao, X. Ji, B. Ruggeri, F. Nees, T. Banaschewski, G. J. Barker, A. L. Bokde, U. Bromberg, C. Buchel, P. J. Conrod, R. Dove, V. Frouin, J. Gallinat, H. Garavan, P. A. Gowland, A. Heinz, B. Ittermann, M. Lathrop, H. Lemaitre, J. L. Martinot, T. Paus, Z. Pausova, J. B. Poline, M. Rietschel, T. Robbins, M. N. Smolka, C. P. Muller, J. Feng, A. Rothenfluh, H. Flor, G. Schumann; IMAGEN Consortium, Neural basis of reward anticipation and its genetic determinants. *Proc. Natl. Acad. Sci. U.S.A.* **113**, 3879–3884 (2016).
24. G. Schumann, E. Loth, T. Banaschewski, A. Barbot, G. Barker, C. Buchel, P. J. Conrod, J. W. Dalley, H. Flor, J. Gallinat, H. Garavan, A. Heinz, B. Itterman, M. Lathrop, C. Mallik, K. Mann, J. L. Martinot, T. Paus, J. B. Poline, T. W. Robbins, M. Rietschel, L. Reed, M. Smolka, R. Spanagel, C. Speiser, D. N. Stephens, A. Strohle, M. Struve; IMAGEN consortium, The IMAGEN study: Reinforcement-related behaviour in normal brain function and psychopathology. *Mol. Psychiatry* **15**, 1128–1139 (2010).
25. J. M. Tyszka, W. M. Pauli, In vivo delineation of subdivisions of the human amygdaloid complex in a high-resolution group template. *Hum. Brain Mapp.* **37**, 3979–3998 (2016).
26. D. M. Dick, G. Smith, P. Olausson, S. H. Mitchell, R. F. Leeman, S. S. O'Malley, K. Sher, Understanding the construct of impulsivity and its relationship to alcohol use disorders. *Addict. Biol.* **15**, 217–226 (2010).
27. S. H. Shin, H. G. Hong, S.-M. Jeon, Personality and alcohol use: The role of impulsivity. *Addict. Behav.* **37**, 102–107 (2012).
28. X. Zhu, C. R. Cortes, K. Mathur, D. Tomasi, R. Momenan, Model-free functional connectivity and impulsivity correlates of alcohol dependence: A resting-state study. *Addict. Biol.* **22**, 206–217 (2017).
29. R. Whelan, R. Watts, C. A. Orr, R. R. Althoff, E. Artiges, T. Banaschewski, G. J. Barker, A. L. Bokde, C. Buchel, F. M. Carvalho, P. J. Conrod, H. Flor, M. Fauth-Buhler, V. Frouin, J. Gallinat, G. Gan, P. Gowland, A. Heinz, B. Ittermann, C. Lawrence, K. Mann, J. L. Martinot, F. Nees, N. Ortiz, M. L. Paillere-Martinot, T. Paus, Z. Pausova, M. Rietschel, T. W. Robbins, M. N. Smolka, A. Strohle, G. Schumann, H. Garavan; IMAGEN Consortium, Neuropsychosocial profiles of current and future adolescent alcohol misusers. *Nature* **512**, 185–189 (2014).
30. S. Peters, J. S. Peper, A. C. K. Van Duijvenvoorde, B. R. Braams, E. A. Crone, Amygdala-orbitofrontal connectivity predicts alcohol use two years later: A longitudinal neuroimaging study on alcohol use in adolescence. *Dev. Sci.* **20**, (2017).
31. J. L. PRICE, Definition of the orbital cortex in relation to specific connections with limbic and visceral structures and other cortical regions. *Ann. N. Y. Acad. Sci.* **1121**, 54–71 (2007).
32. R. L. Cook, T. Chung, T. M. Kelly, D. B. Clark, Alcohol screening in young persons attending a sexually transmitted disease clinic: Comparison of AUDIT, CRAFFT, and CAGE instruments. *J. Gen. Intern. Med.* **20**, 1–6 (2005).
33. D. Garcia, N. Lester, K. M. Cloninger, C. R. Cloninger, V. Zeigler-Hill, T. Shackelford, The temperament and character inventory (TCI). *Encyclopedia of personality and individual differences. Cham: Springer*, 1–3 (2017).
34. R. Goodman, The strengths and difficulties questionnaire: A research note. *J. Child Psychol. Psychiatry* **38**, 581–586 (1997).
35. H. Vulser, H. Lemaitre, E. Artiges, R. Miranda, J. Penttila, M. Struve, T. Fadai, V. Kappel, Y. Grimmer, R. Goodman, A. Stringaris, L. Poustka, P. Conrod, V. Frouin, T. Banaschewski, G. J. Barker, A. L. Bokde, U. Bromberg, C. Buchel, H. Flor, J. Gallinat, H. Garavan, P. Gowland, A. Heinz, B. Ittermann, C. Lawrence, E. Loth, K. Mann, F. Nees, T. Paus, Z. Pausova, M. Rietschel, T. W. Robbins, M. N. Smolka, G. Schumann, J. L. Martinot, M. L. Paillere-Martinot; IMAGEN Consortium (www.imagen-europe.com), Subthreshold depression and regional brain volumes in young community adolescents. *J. Am. Acad. Child Adolesc. Psychiatry* **54**, 832–840 (2015).
36. B. Knutson, G. W. Fong, C. M. Adams, J. L. Varner, D. Hommer, Dissociation of reward anticipation and outcome with event-related fMRI. *Neuroreport* **12**, 3683–3687 (2001).
37. R. H. R. Pruim, M. Mennes, D. van Rooij, A. Llera, J. K. Buitelaar, C. F. Beckmann, ICA-AROMA: A robust ICA-based strategy for removing motion artifacts from fMRI data. *NeuroImage* **112**, 267–277 (2015).
38. Y. Behzadi, K. Restom, J. Liau, T. T. Liu, A component based noise correction method (CompCor) for BOLD and perfusion based fMRI. *NeuroImage* **37**, 90–101 (2007).
39. S. Whitfield-Gabrieli, A. Nieto-Castanon, Conn: A functional connectivity toolbox for correlated and anticorrelated brain networks. *Brain Connect.* **2**, 125–141 (2012).

Acknowledgments

Funding: This work received support from the following sources: National Key R&D Program of China (no. 2019YFA0709501, no. 2018YFC1312900, and no. 2019YFA0709502), the National Natural Science Foundation of China (no. 81801773), the Shanghai Pujiang Project (no. 18PJ1400900), the European Union-funded FP6 Integrated Project IMAGEN

(Reinforcement-related behaviour in normal brain function and psychopathology) (LSHM-CT-2007-037286), the Horizon 2020–funded ERC Advanced Grant "STRATIFY" (Brain network based stratification of reinforcement-related disorders) (695313), the 111 Project (No. B18015) and the National Natural Science Foundation of China (no. 91630314), the key project of Shanghai Science and Technology (no. 16JC1420402), Shanghai Municipal Science and Technology Major Project (no. 2018SHZDZX01), ZJ Lab, ERANID (Understanding the Interplay between Cultural, Biological and Subjective Factors in Drug Use Pathways) (PR-ST-0416-10004), Human Brain Project (HBP SGA 2, 785907, and HBP SGA 3, 945539), the Medical Research Council Grant "c-VEDA" (Consortium on Vulnerability to Externalizing Disorders and Addictions) (MR/N000390/1), the NIH (R01DA049238, A decentralized macro and micro gene-by-environment interaction analysis of substance use behavior and its brain biomarkers), the National Institute for Health Research (NIHR) Biomedical Research Centre at South London and Maudsley N.H.S. Foundation Trust and King's College London, the Bundesministeriumfür Bildung und Forschung (BMBF grants 01GS08152 and 01EV0711; Forschungsnetz AERIAL 01EE1406A and 01EE1406B), the Deutsche Forschungsgemeinschaft (DFG grants SM 80/7-2, SFB 940, TRR 265, and NE 1383/14-1), the Medical Research Foundation and Medical Research Council (grants MR/R00465X/1 and MR/S020306/1), and the NIH-funded ENIGMA (grants 5U54EB020403-05 and 1R56AG058854-01). Further support was provided by grants from the ANR (ANR-12-SAMA-0004 and AAPG2019, GeBra), the Eranet Neuron (AF12-NEUR0008-01, WM2NA; ANR-18-NEUR00002-01, ADORe), the Fondation de France (00081242), the Fondation pour la Recherche Médicale (DPA20140629802), the Mission Interministérielle de Lutte-contre-les-Drogues-et-les-Conduites-Addictives (MILDECA), the Assistance-Publique-Hôpitaux-de-Paris and INSERM (interface grant), the Paris Sud University IDEX 2012, the Fondation de l'Avenir (grant AP-RM-17-013), the Fédération pour la Recherche sur le Cerveau, the NIH, Science Foundation Ireland (16/ERCD/3797), USA (Axon, Testosterone and Mental Health during Adolescence; RO1 MH085772-01A1), and the NIH Consortium grant U54 EB020403, supported by a cross-NIH alliance that funds Big Data to Knowledge Centres of Excellence. **Author contributions:** T.J., T.W.R., and J.F. conceptualized the study. T.J., C.X., and T.W.R. wrote the manuscript. T.J. and C.X. analyzed the data. T.B., G.J.B., A.L.W.B., C.B., S.D., J.F., H.F., A.G., H.G., P.G., A.H., B.I., J.-L.M., M.-L.P.M., F.N., L.P., J.H.F., M.N.S., H.W., R.W., and G.S. were the principal investigators of IMAGEN. E.B.Q., T.B., G.J.B., A.L.W.B., C.B., H.F., A.G., H.G., P.G., A.H., B.I., J.-L.M., M.-L.P.M., F.N., D.P.O., L.P., J.H.F., M.N.S., H.W., R.W., and G.S. acquired the data. All authors critically revised the manuscript. **Competing interests:** T.B. served in an advisory or consultancy role for Lundbeck, Medice, Neurim Pharmaceuticals, Oberberg GmbH, and Shire. He received conference support or speaker's fee by Lilly, Medice, Novartis, and Shire. He has been involved in clinical trials conducted by Shire and Viforpharma. He received royalties from Hogrefe, Kohlhammer, C.I.P. Medien, and Oxford University Press. G.J.B. has received honoraria from General Electric Healthcare for teaching on scanner programming courses. L.P. served in an advisory or consultancy role for Roche and Viforpharm and received speaker's fee by Shire. She received royalties from Hogrefe, Kohlhammer, and Schattauer. The present work is unrelated to the above grants and relationships. The other authors declare that they have no competing interests. **Data and materials availability:** IMAGEN data are available from a dedicated database: https://imagen2.cea.fr. Custom code that supports the findings of this study is available from the corresponding author upon request. All data needed to evaluate the conclusions in the paper are present in the paper and/or the Supplementary Materials. Additional data related to this paper may be requested from the authors.

Submitted 18 June 2020
Accepted 16 December 2020
Published 3 February 2021
10.1126/sciadv.abd4074

Citation: T. Jia, C. Xie, T. Banaschewski, G. J. Barker, A. L. W. Bokde, C. Büchel, E. B. Quinlan, S. Desrivières, H. Flor, A. Grigis, H. Garavan, P. Gowland, A. Heinz, B. Ittermann, J.-L. Martinot, M.-L. P. Martinot, F. Nees, D. P. Orfanos, L. Poustka, J. H. Fröhner, M. N. Smolka, H. Walter, R. Whelan, G. Schumann, T. W. Robbins, J. Feng, IMAGEN Consortium, Neural network involving medial orbitofrontal cortex and dorsal periaqueductal gray regulation in human alcohol abuse. *Sci. Adv.* **7**, eabd4074 (2021).

ScienceAdvances

Neural network involving medial orbitofrontal cortex and dorsal periaqueductal gray regulation in human alcohol abuse

Tianye JiaChao XieTobias BanaschewskiGareth J. BarkerArun L. W. BokdeChristian BüchelErin Burke QuinlanSylvane DesrivièresHerta FlorAntoine GrigisHugh GaravanPenny GowlandAndreas HeinzBernd IttermannJean-Luc MartinotMarie-Laure Paillère MartinotFrauke NeesDimitri Papadopoulos OrfanosLuise PoustkaJuliane H. FröhnerMichael N. SmolkaHenrik WalterRobert WhelanGunter SchumannTrevor W. RobbinsJianfeng Feng

Sci. Adv., 7 (6), eabd4074. • DOI: 10.1126/sciadv.abd4074

Science Advances (ISSN 2375-2548) is published by the American Association for the Advancement of Science. 1200 New York Avenue NW, Washington, DC 20005. The title *Science Advances* is a registered trademark of AAAS.